

Overview of the recent results of the RT-1 magnetospheric experiment with levitated superconducting coil

H. Saitoh, Z. Yoshida, J. Morikawa, Y. Yano, T. Mizushima, and M. Kobayashi
University of Tokyo, JAPAN

1. Introduction: Magnetospheric plasma device RT-1
2. Formation of high- β ECH plasma
 - improved plasma parameters, x-ray camera imaging
3. Confinement of toroidal pure electron plasma
 - long time (~ 300 s) trap, inward particle diffusion
4. Summary and future tasks

ICC2010 workshop, 16-19 Feb 2010, Princeton

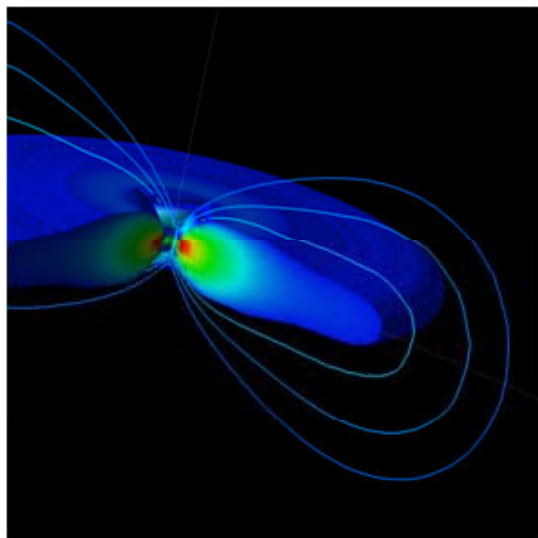


新領域創成科学研究科基盤科学研究系
Transdisciplinary Sciences, GSFS



東京大学
THE UNIVERSITY OF TOKYO

1. Introduction: Magnetospheric plasma experiment 2/20

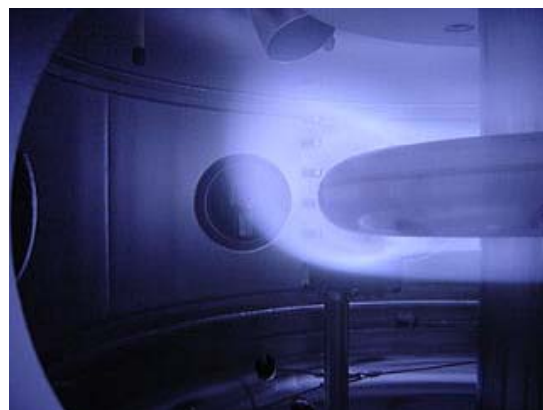
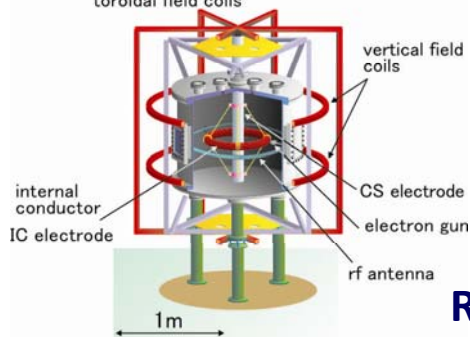


High- β flowing plasma near Jupiter

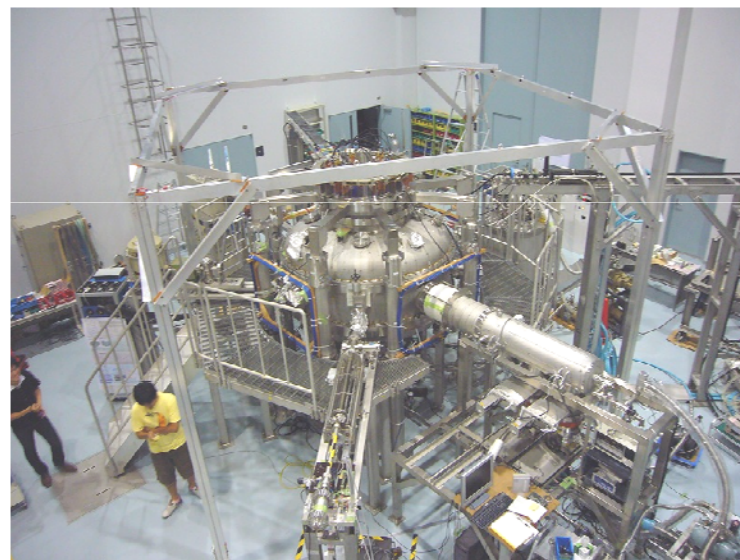
- Stable confinement configuration for high- β plasma is essential for advanced fusion concept.
- Spacecraft observations shows existence of **flowing high- β plasma** in **Jovian magnetosphere**.
- Taking a hint from the astrophysical phenomenon, dipole fusion experiments started: **LDX** and **RT**
- Ultra high- β state (possibly >1) due to the **dynamic pressure of fast flow** is theoretically predicted.



toroidal field coils



Proto-RT and Mini-RT
(1998-) (2003-)



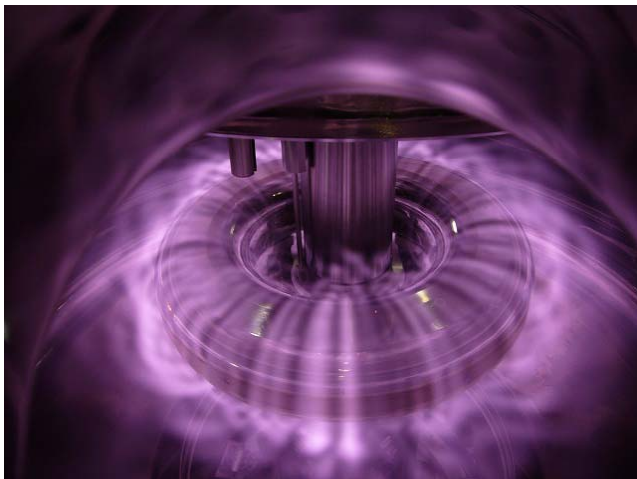
Ring Trap 1 (RT-1)
(2006-)

RT Experiments at University of Tokyo, JAPAN

Hasegawa *et al.*, Nucl. Fusion **30**, 2405 (1990).

RT1: Yoshida *et al.*, PRL **88**, 095001 (2002); PFR **1**, 008 (2006), LDX: Garnier *et al.*, Phys. Plasmas **13**, 056111 (2006).

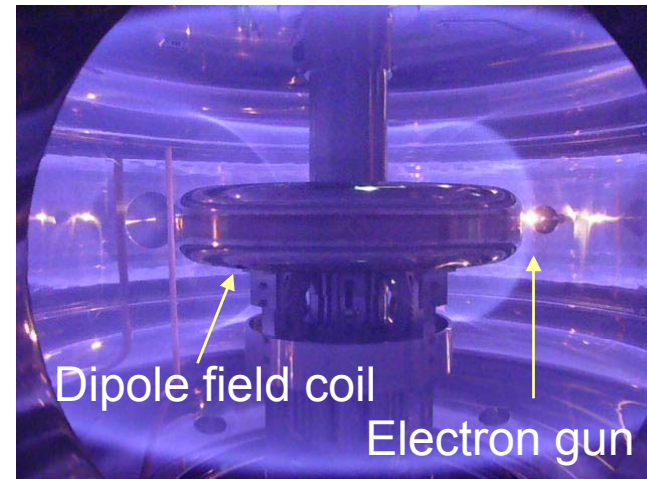
- **High- β plasma confinement in a magnetospheric configuration**
 - Suitable for burning **advanced fusion** fuels, such as D-D or D-3He
 - Physics of flowing plasmas (flow formation is not conducted at present)
- **Stable confinement of toroidal non-neutral plasma**
 - Capable of trapping plasmas with arbitrary non-neutrality
 - Potential applications for antimatter plasmas (currently only electrons)



ECH plasma generated by 2.45GHz RF

ECH plasma

- Improved plasma by coil levitation
- Local β value $\sim 40\%$ (hot electrons)
- SX CCD camera, etc.



Electron beam injection by electron gun

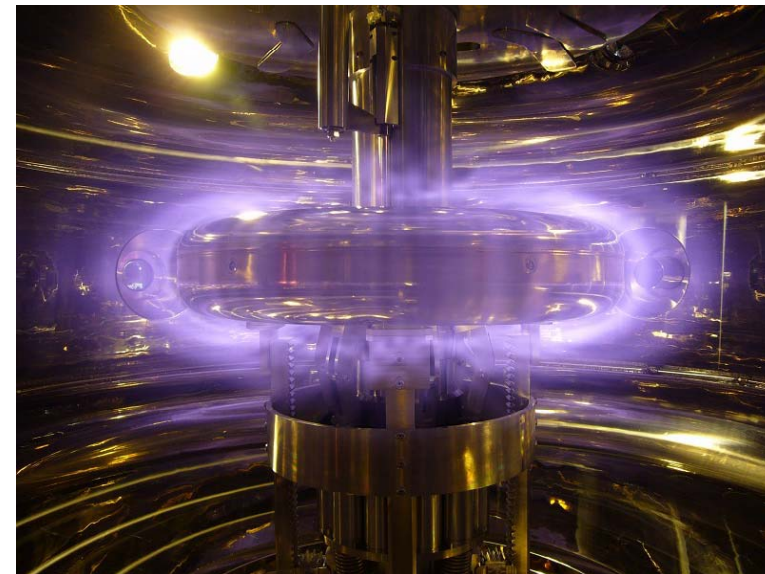
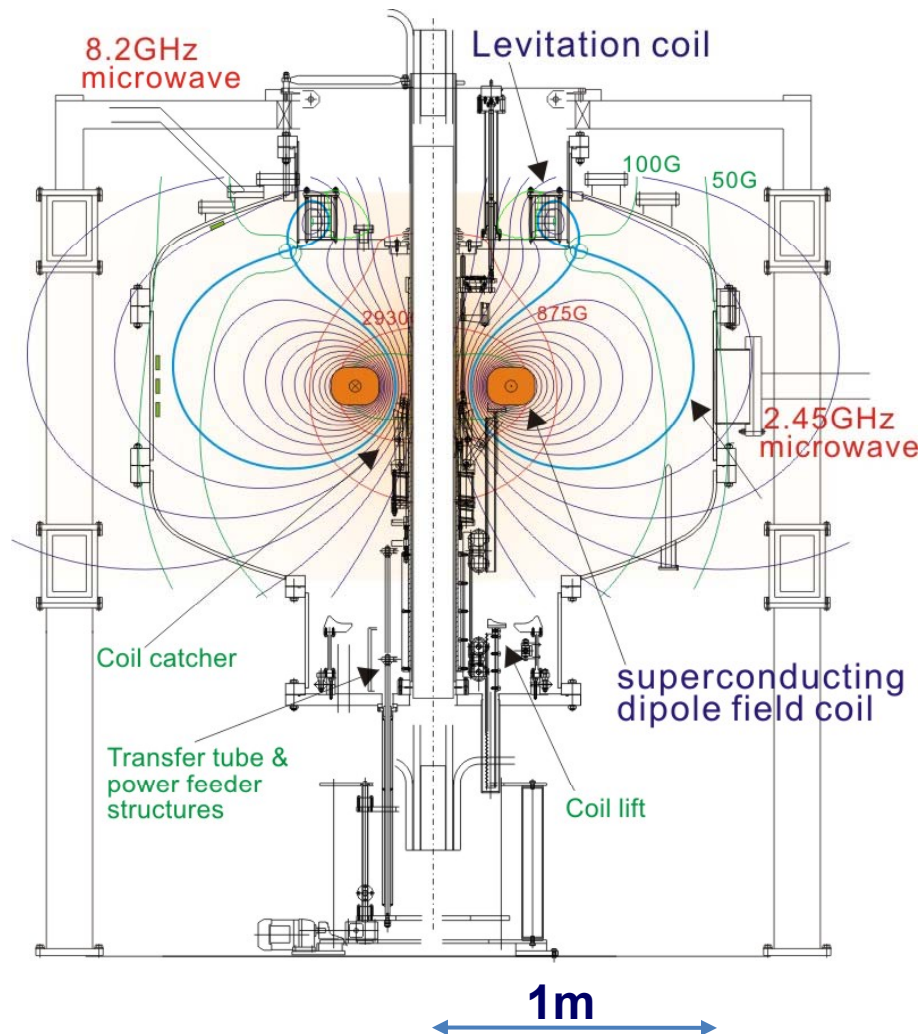
Non-neutral (pure electron) plasma

- Confinement time exceeds 300s
- Inward particle diffusion was observed
- Stable oscillation suggests rigid-rotation

*Yoshida, Ogawa *et al.*, in *Non-neutral Plasma Physics III* (AIP 1999); Ogawa *et al.*, PFR 4, 020 (2009).

The Ring Trap 1 (RT-1) device

4/20

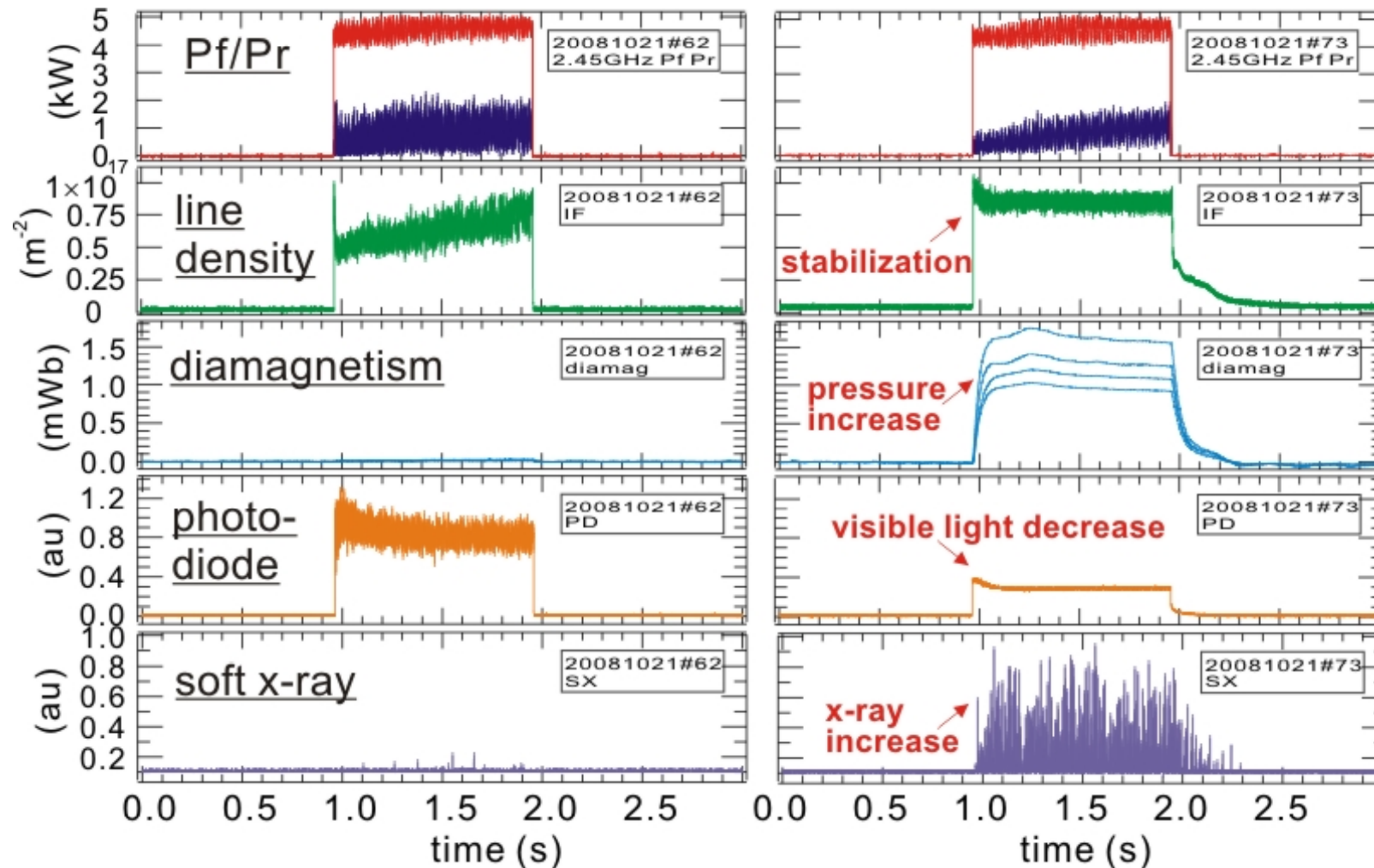


Cross section of RT-1: Magnetospheric configuration generated by a levitated High- T_c (Bi-2223) superconducting coil

- Plasma formation by ECH
 - 2.45GHz (20kW) and 8.2GHz (25kW)
- Diagnostic system includes
 - 75GHz (4mm) interferometer
 - Visible light spectroscopy
 - Diamag loops and magnetic probes
 - SiLi and CdTe x-ray detectors
 - Soft x-ray CCD camera
 - Edge Langmuir probes

2. High β (hot electron) plasma formation

5/20

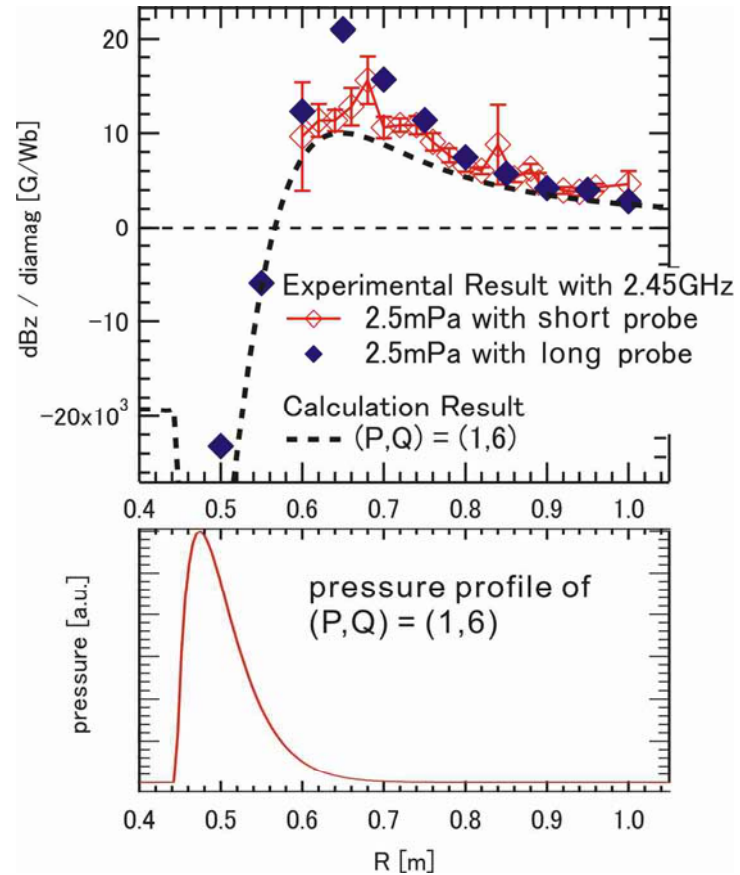
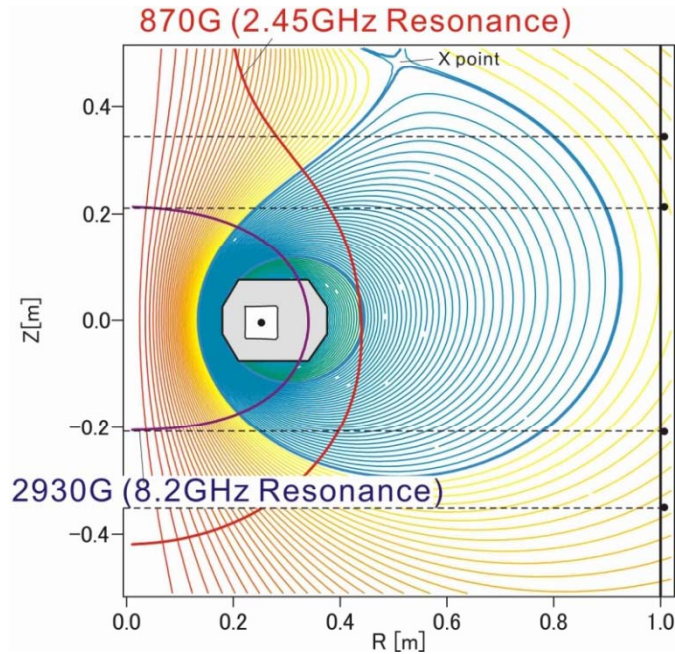


Typical wave forms with 2.45GHz ECH plasma (a) $P_{H_2} = 4.5 \times 10^{-2} \text{ Pa}$ (b) $1.3 \times 10^{-3} \text{ Pa}$.

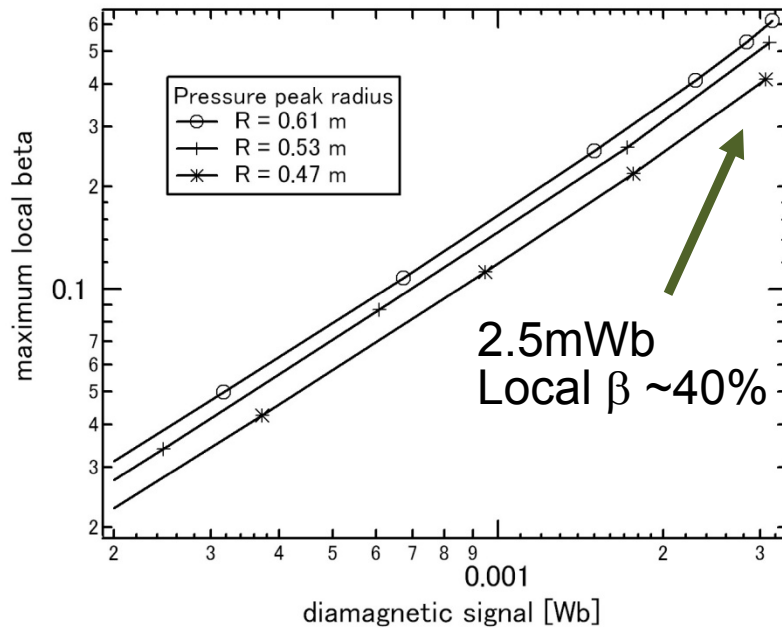
- By optimizing neutral gas pressure, high- β plasma is generated.
- Plasma pressure mainly results from hot component ($T_e \sim 10 \text{ keV}$; SiLi detectors).

Grad-Shafranov equilibrium analysis

6/20



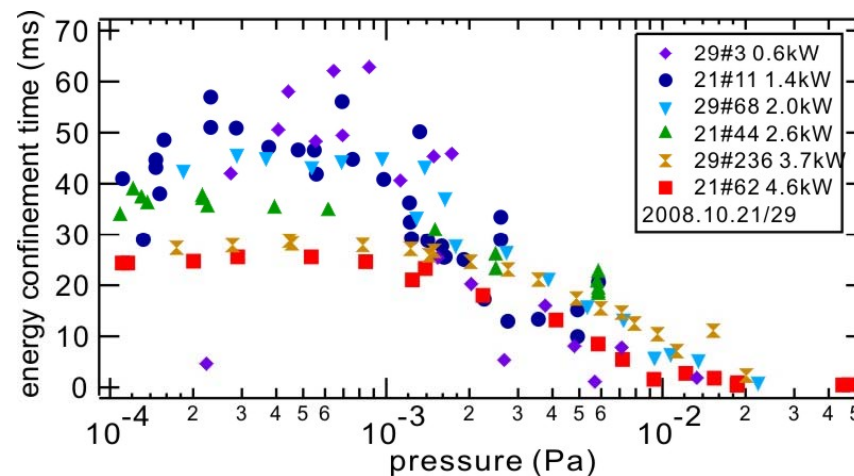
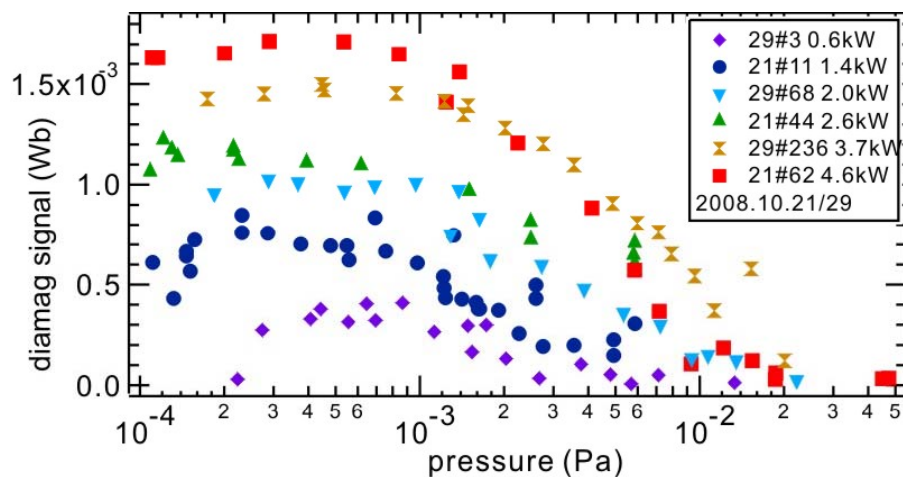
Y. Yano,
to be
submitted.



- Diamag loop signal and local β values
- Pressure profiles have steep gradient near the superconducting coil.

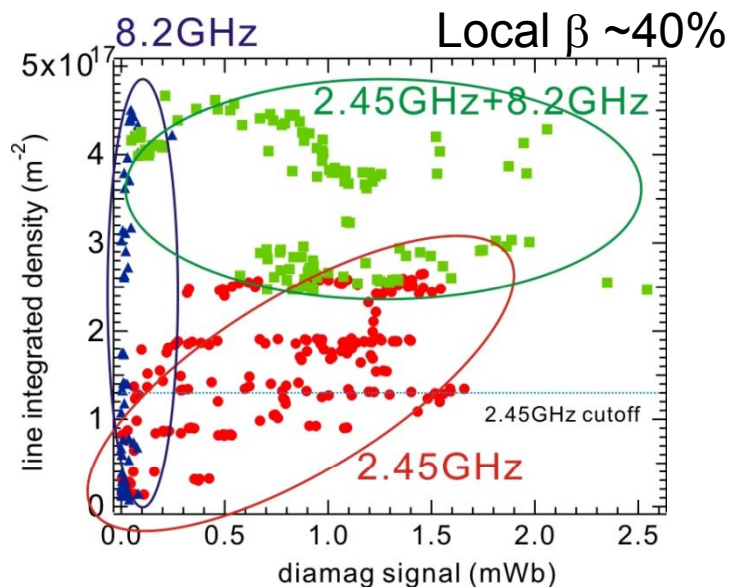
Energy confinement time and β values

7/20



Plasma pressure (diamagnetic signal) and energy confinement time

- Hot electron population reaches $\sim 30\%$ by reducing neutral gas pressure.

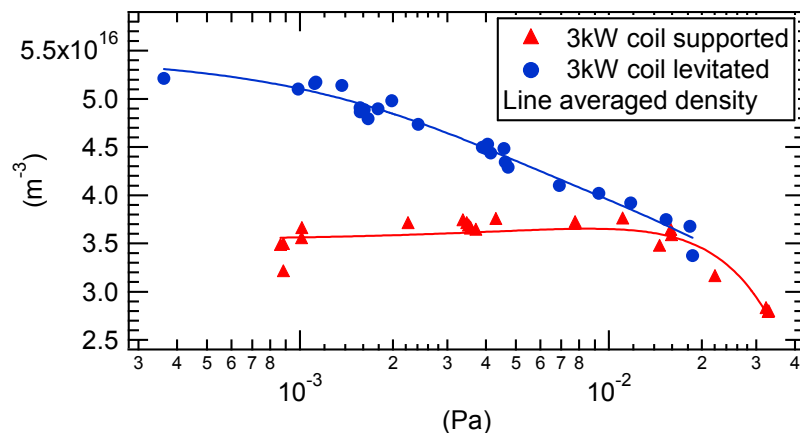
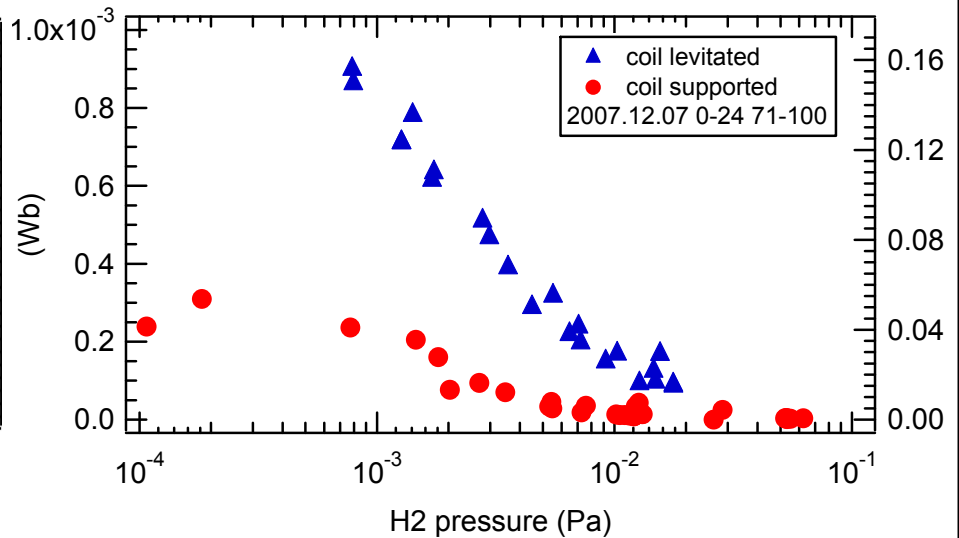
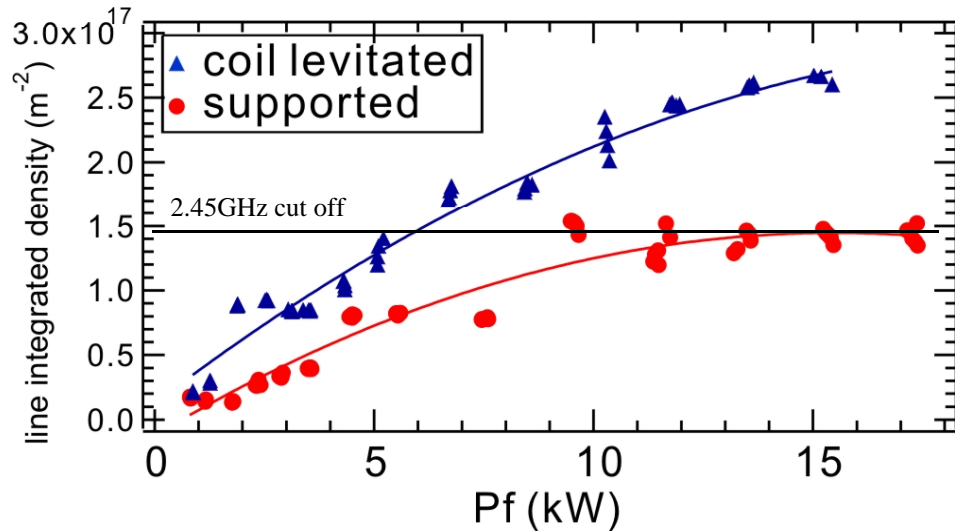


Diamag-Ne, 8.2/2.45GHz ECH

- Energy confinement time estimated from from stored energy and injected RF power is $\tau_{e1} \sim 60\text{ms}$.
- τ_{e1} approximately agrees with magnetic measurement (diamag-decay time) of $\tau_{e2} \sim 100\text{ms}$.
- The stored energy is typically higher for 2.45GHz ECH

Improvement by coil levitation

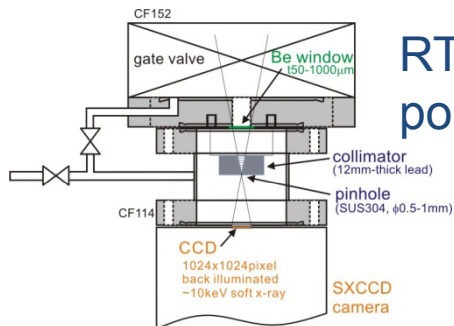
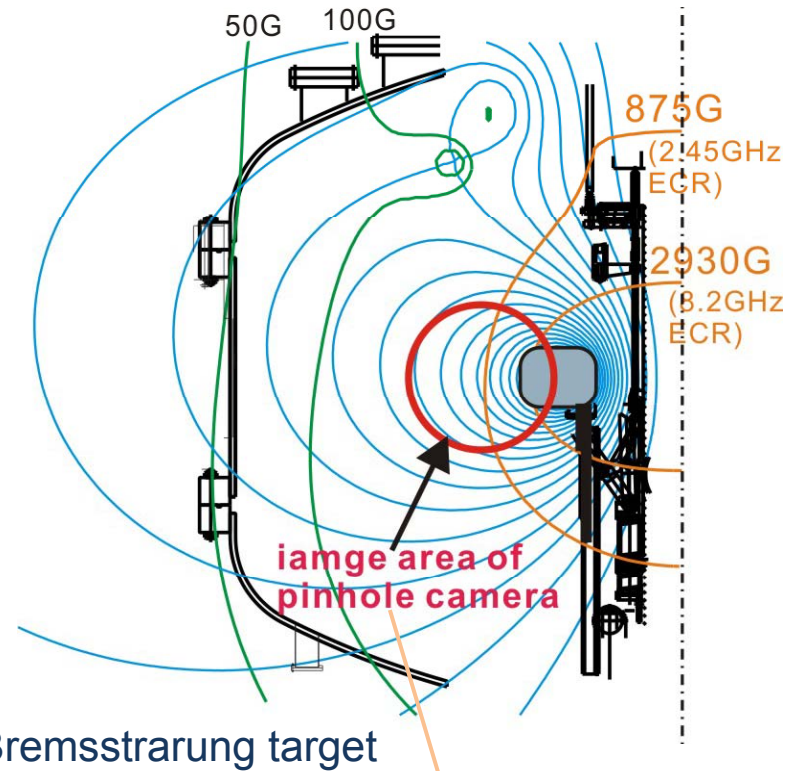
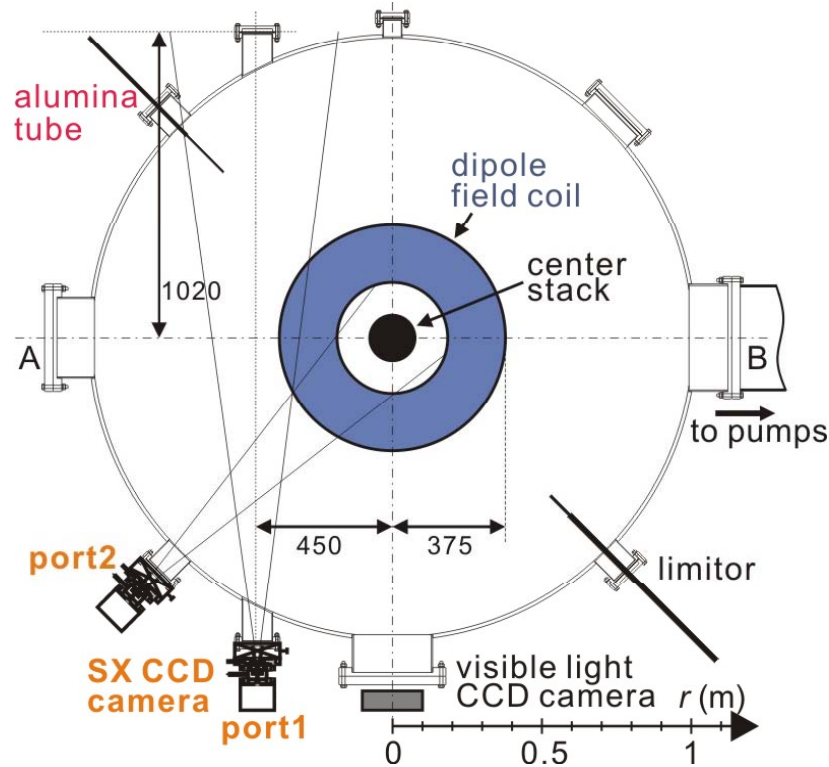
8/20



➤ Electron densities

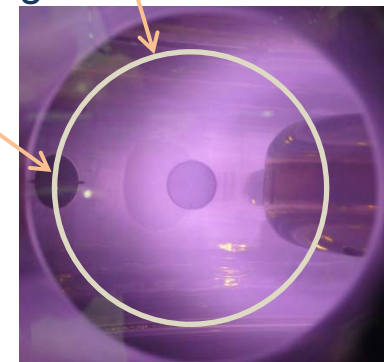
- by 75GHz interferometer (1ch).
- Loss by coil support minimized, two times higher density realized.
- Ne exceeds cut off density, (mode conversion to EBW).

Hot electron imaging by x-ray CCD camera 9/20



RT-1 cross section, camera (ceramic tube) ports, and camera construction.

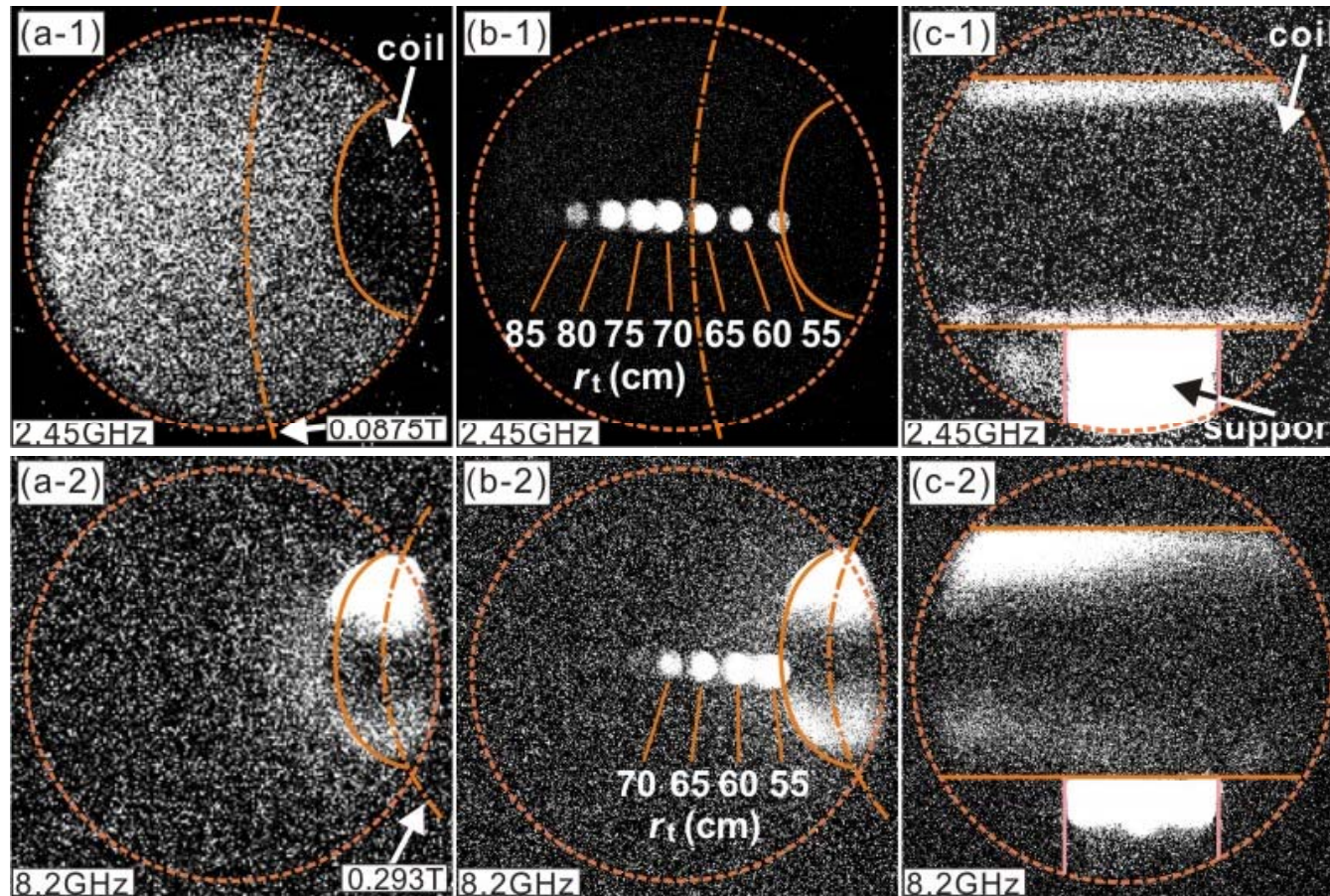
Visible light image from port 1



Visible light view from port 1

➤ Soft x-ray CCD camera

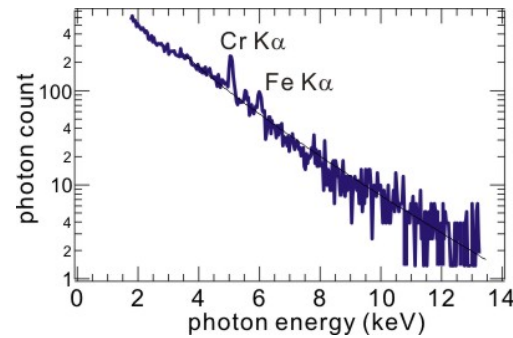
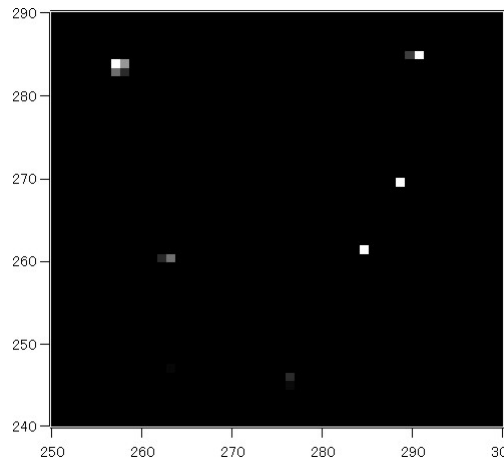
- 1024 \times 1024 pixel (13 \times 13mm), 16bit dynamic range
- Be window (100 μ m), collimator, tantalum pinhole



Soft x-ray images observed from (a) port 1, (b) port 1 with insertion of target tube At different radial positions, and (c) port2. (1) 2.45GHz and (b) 8.2GHz ECH.

- · 2.45GHz: hot electrons fill approximately entire region in the image circle
- 8.2GHz: x-ray emitting region localized near the coil, some lost on coil surface
- Relatively large diamagnetic signal observed for 2.45GHz rather than 8.2GHz.
- Coil support structure is the main loss channel of hot electrons for both cases

Measurement of T_e by photon counting mode 11/20

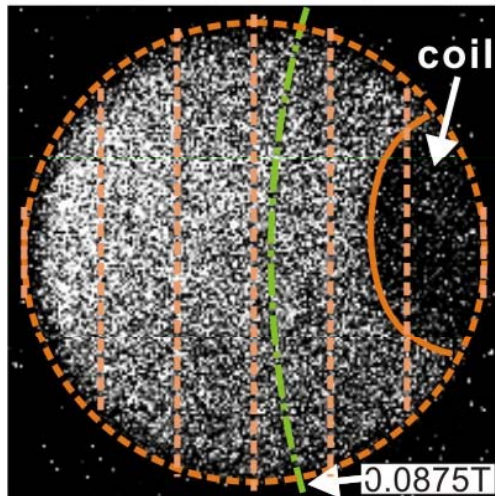


Enlarged CCD image and pulse height analysis

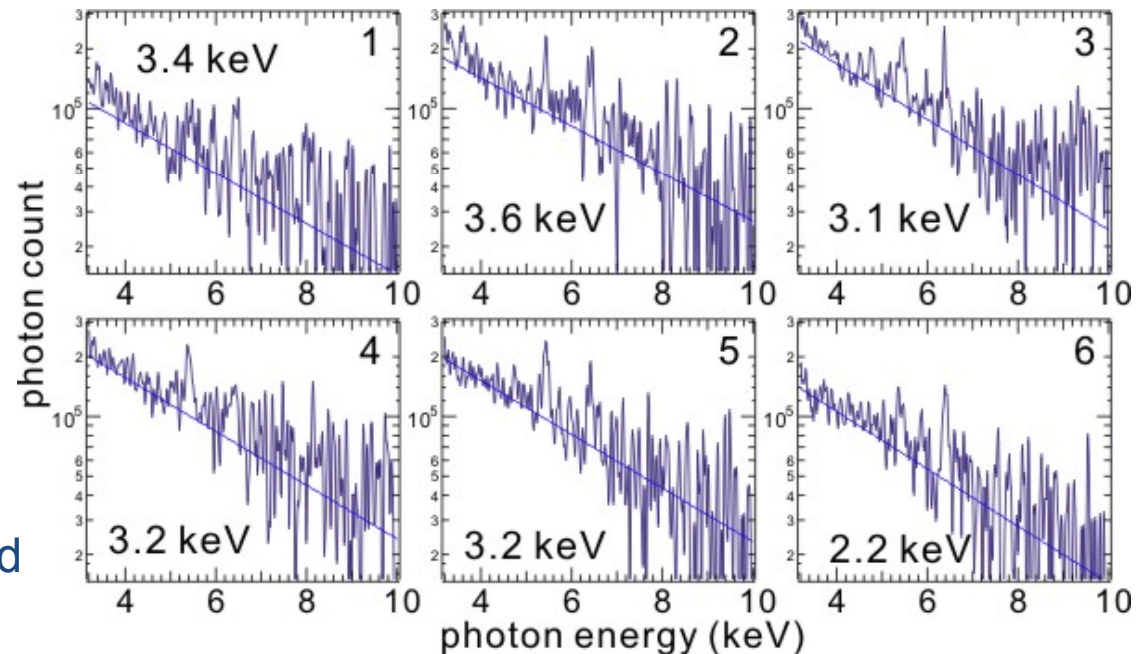
- Pulse height analysis of photon energies with CCD
- Impurity lines are used for energy calibration
- T_e is approximately constant in the image circle...
- Experiment with coil levitation is future task

Preliminary results without coil levitation

1 2 3 4 5 6



Separated image region and photon energy spectrum



* Y. Liang *et al.*, Rev. Sci. Instrum. **72**, 717 (2001), H. Saitoh *et al.*, PFR **4**, 050 (2009).

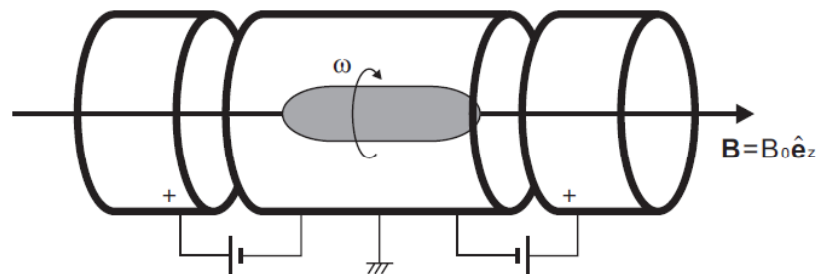
Magnetosheric toroidal non-neutral plasma 12/20

- **Studies of particle transport properties in RT-1 using NNP**
 - **Inward particle diffusion** is predicted and observed in magnetospheres.
 - fluctuation-induced transport realized by violating the 3rd invariant.
 - resultant steep density gradient and adiabatic heating predicted.
 - Inward transport of particles are observed in RT-1 using NNP.

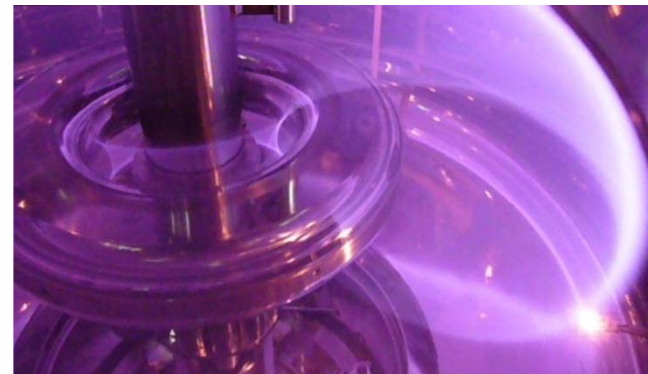
A. Hasegawa, *Comm. Plasma Phys. Cntrl. Fusion* 1, 147 (1987); LDX, RT-1

- **Toroidal non-neutral plasmas**
 - Non-neutral plasma in strongly inhomogeneous magnetic field.
 - Capable of trapping **plasmas with arbitrary non-neutrality**.
 - Potential applications for antimatter plasmas (currently only electrons).

RT-1, Columbia Non-neutral Torus, Lawrence Non-neutral Torus II

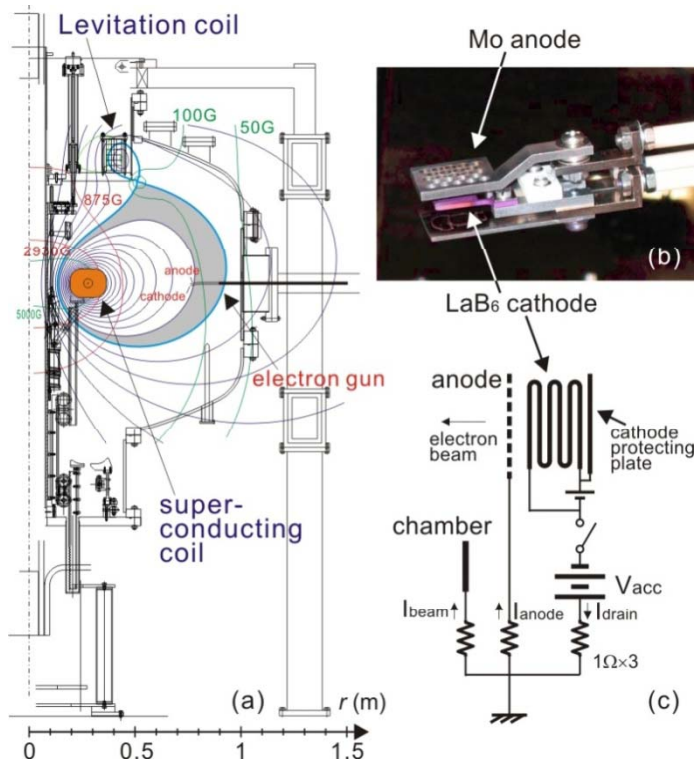


Linear configuration for non-neutral Plasmas (Penning-malmberg trap, etc.)

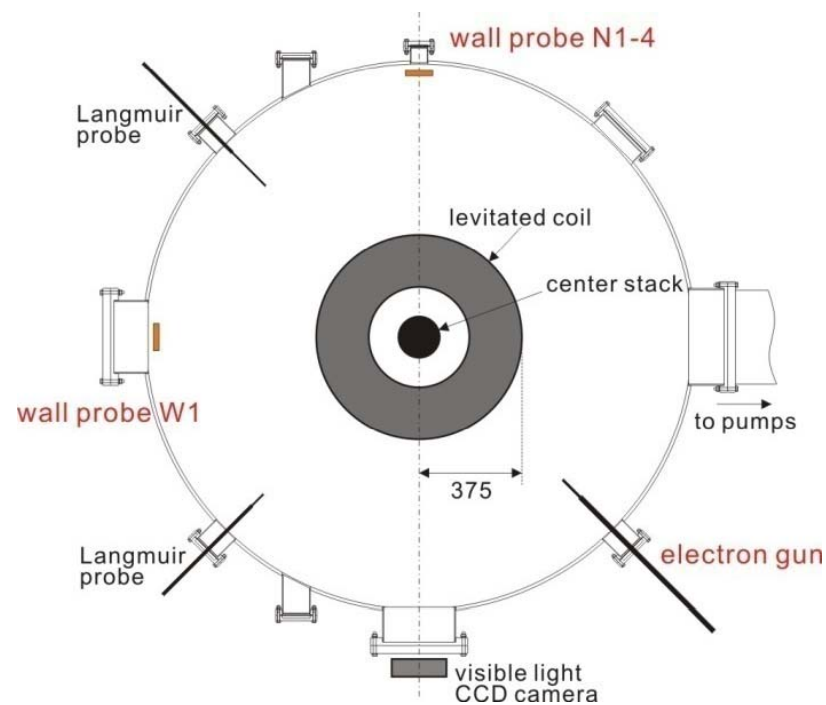


Toroidal configuration requires no axial potential well for confinement.

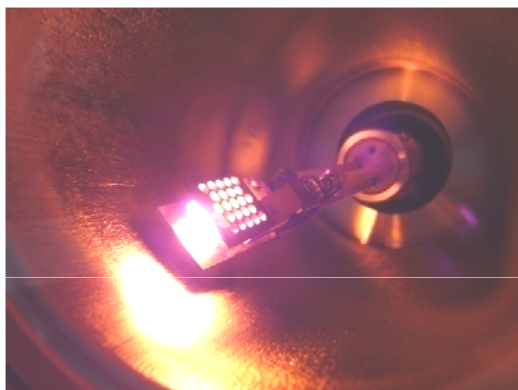
Electron beam injection & plasma formation 13/20



Cross-section of RT-1 and Electron gun construction

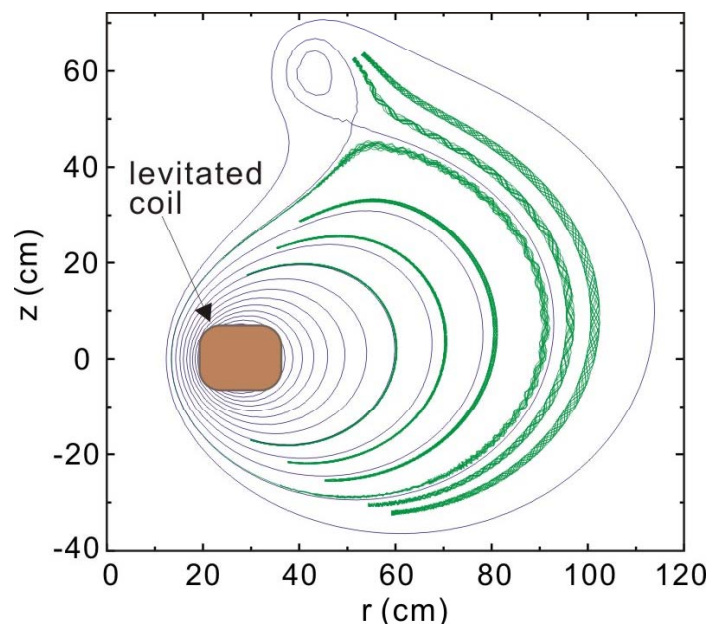


Top view of RT-1 including electron gun, Wall probes, and Langmuir probe for pure electron plasma experiment



- Electrons are injected into static fields, from an electron gun located at the edge region.
- Electrons are initially accelerated between LaB_6 hot cathode ($-V_{\text{acc}}$) and molybdenum anode (0V).

Electron injection and visualized magnetic surfaces 14/20

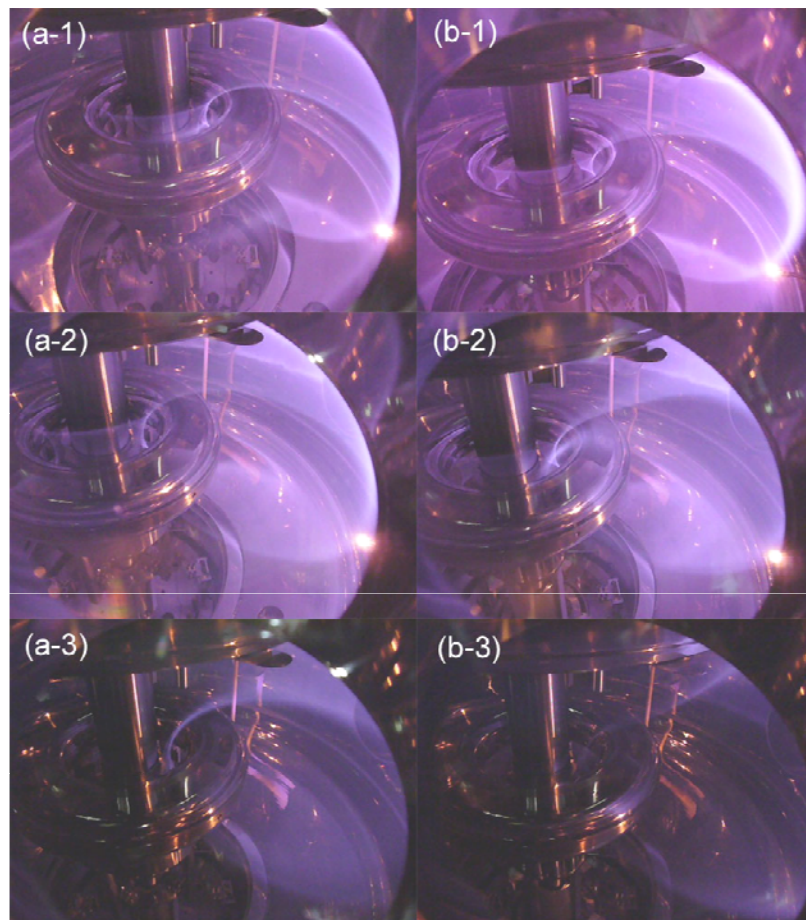


Single-particle orbits of electron
Projected on r-z cross section of RT-1

$$P_\theta = \frac{\partial L}{\partial \dot{\theta}} = mr^2 \dot{\theta} + qrA_\theta = \text{const.}$$

$$L = \frac{mv^2}{2} + q\mathbf{v} \cdot \mathbf{A} - q\phi$$

$$d \leq \left| \frac{mr\dot{\theta}}{qB_p} \right|$$

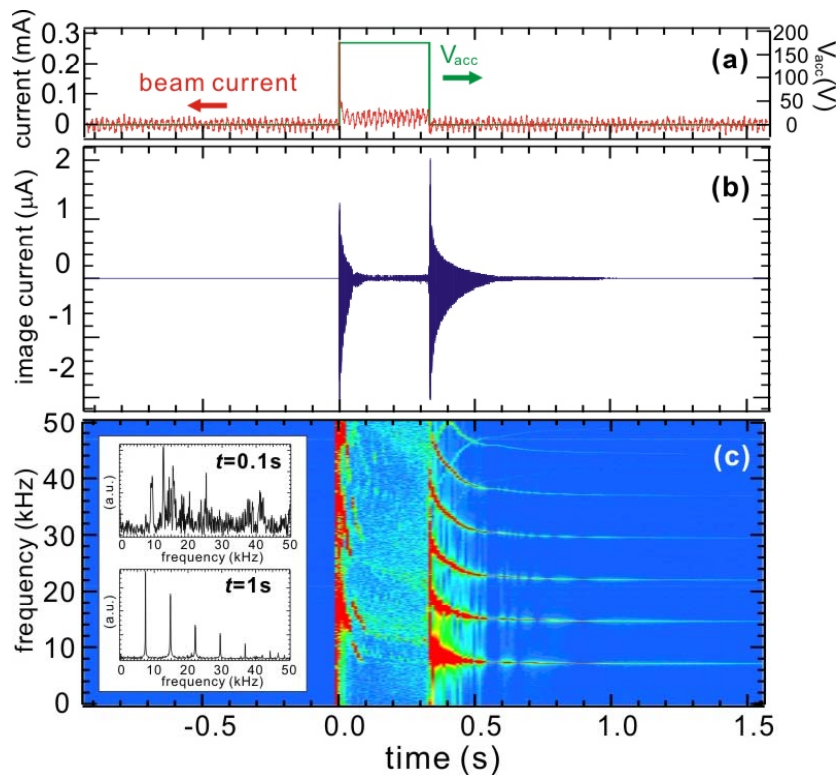


Visualized magnetic surfaces by electron injection
Into filled gas (a) without and (b) with coil levitation

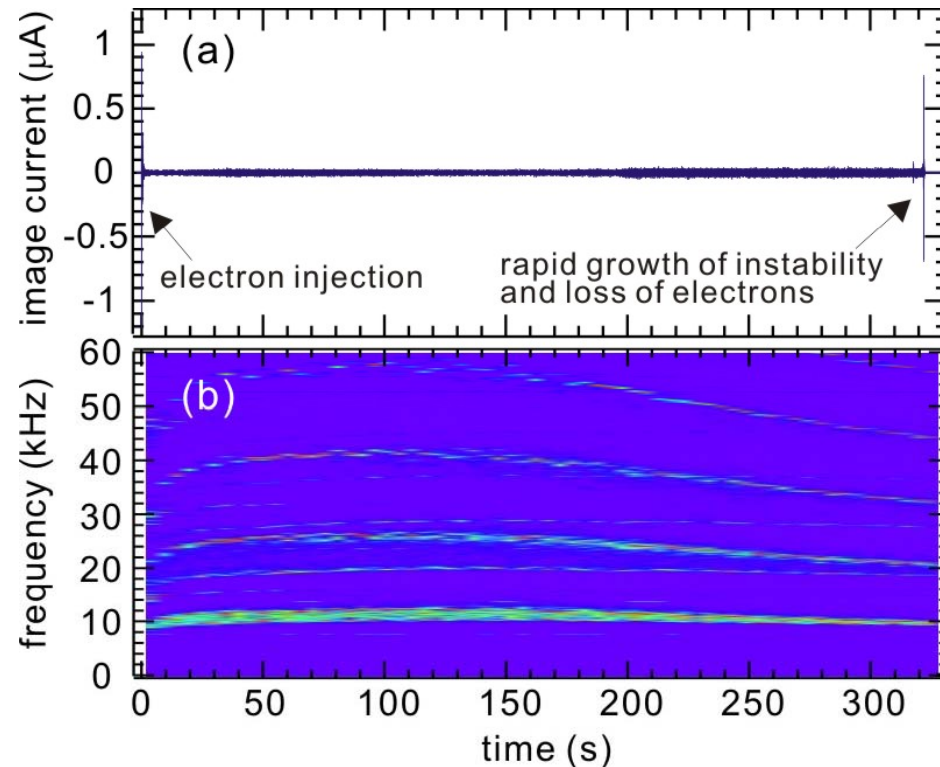
- In pure poloidal field of RT-1, single particle orbits are localized near the initial magnetic surfaces ($r_L < 6\text{mm}$).
- Visualized surfaces agrees with calculated vacuum magnetic surfaces.

Observation of long confinement

15/20

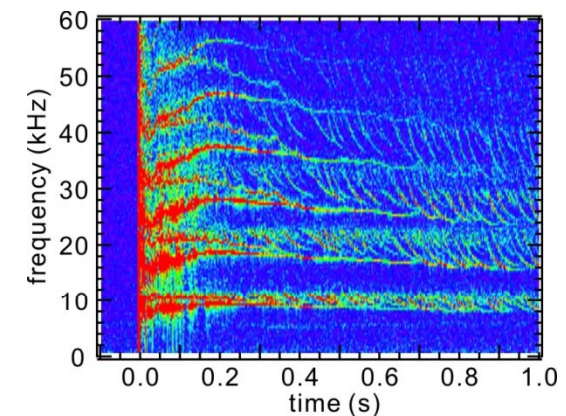


Waveforms during and just after beam injection



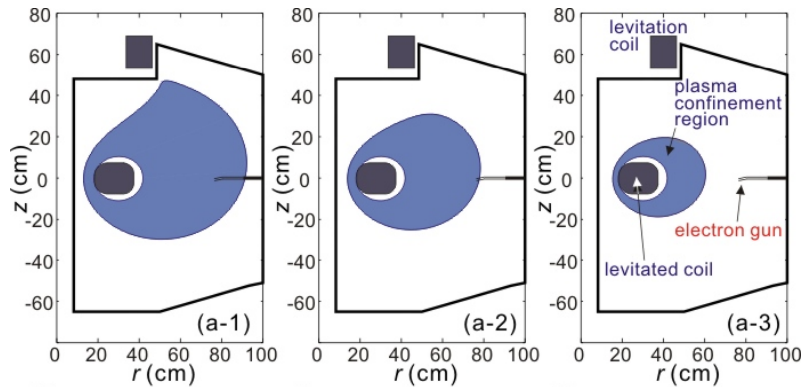
Fluctuation during long confinement

- The fluctuation spectrum has large-amplitude, broad, and multiple peaks during electron injection.
- After beam supply ends, fluctuation stabilizes and the plasma is trapped for more than 300s.
- Coherent fluctuation suggests rigid rotation, in spite of strongly inhomogeneous field strength.

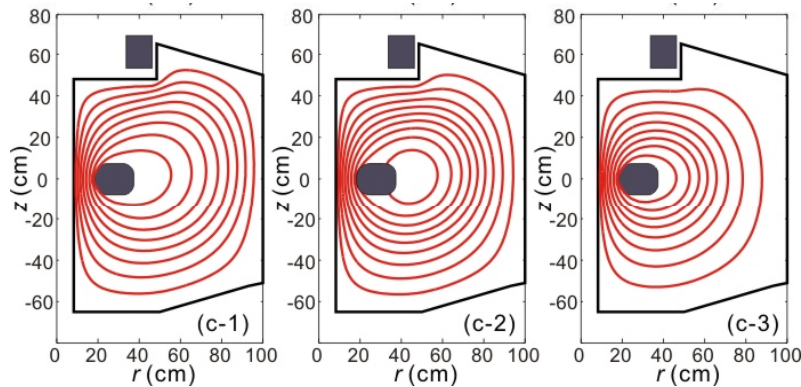


Frequency repeatedly drops

Inward particle diffusion (electron confinement region)

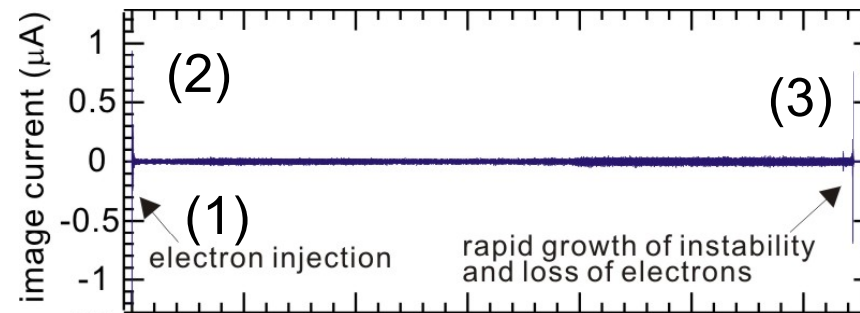


Estimated confinement regions of (1) during electron injection (2) just after injection ends (3) just before confinement ends. (Most well-reconstructing the wall probe measurements, $N_e \sim 10^{11} \text{m}^{-3}$.)



Space potential profiles for the three phases.

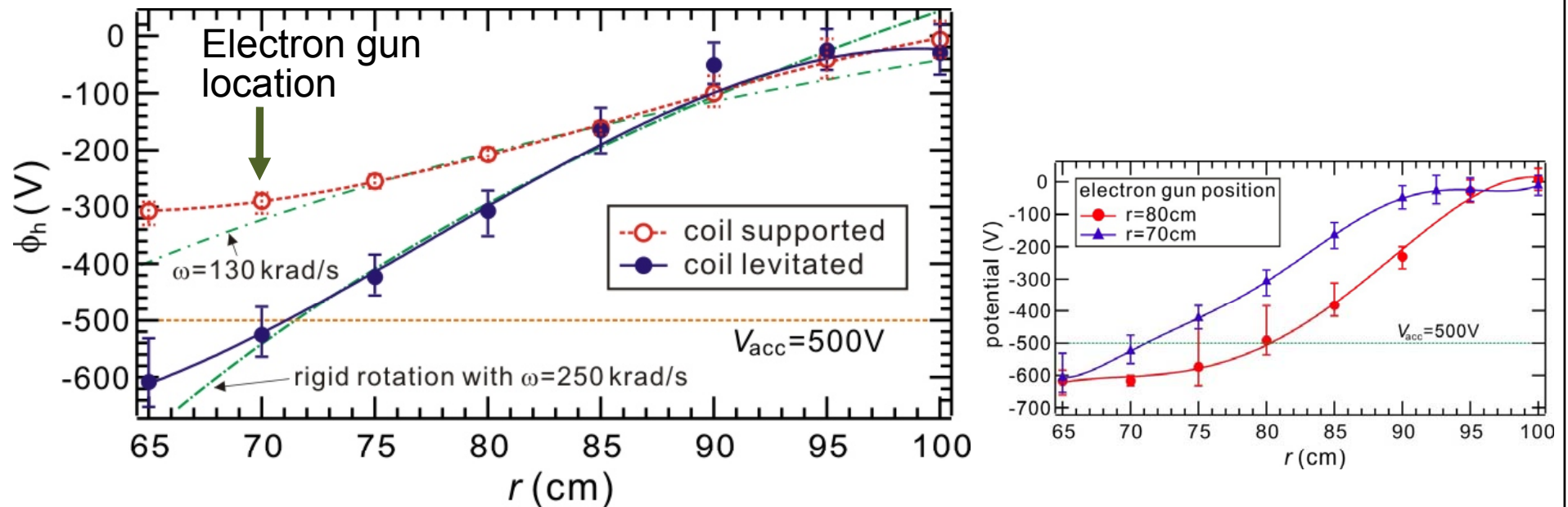
➤ Confinement regions are estimated using wall probes (methods reported in poster).



➤ Confinement region gradually shifts inward:

- During beam injection, approximately whole region inside the separatrix are filled.
 - Plasma on magnetic surfaces intersecting the gun structure is rapidly lost.
 - Plasma stably trapped in strong field region.
- Electrons deviates from initial magnetic surfaces, transported to strong field region.

Potential profiles (energy increase of collisionless electrons) 17/20

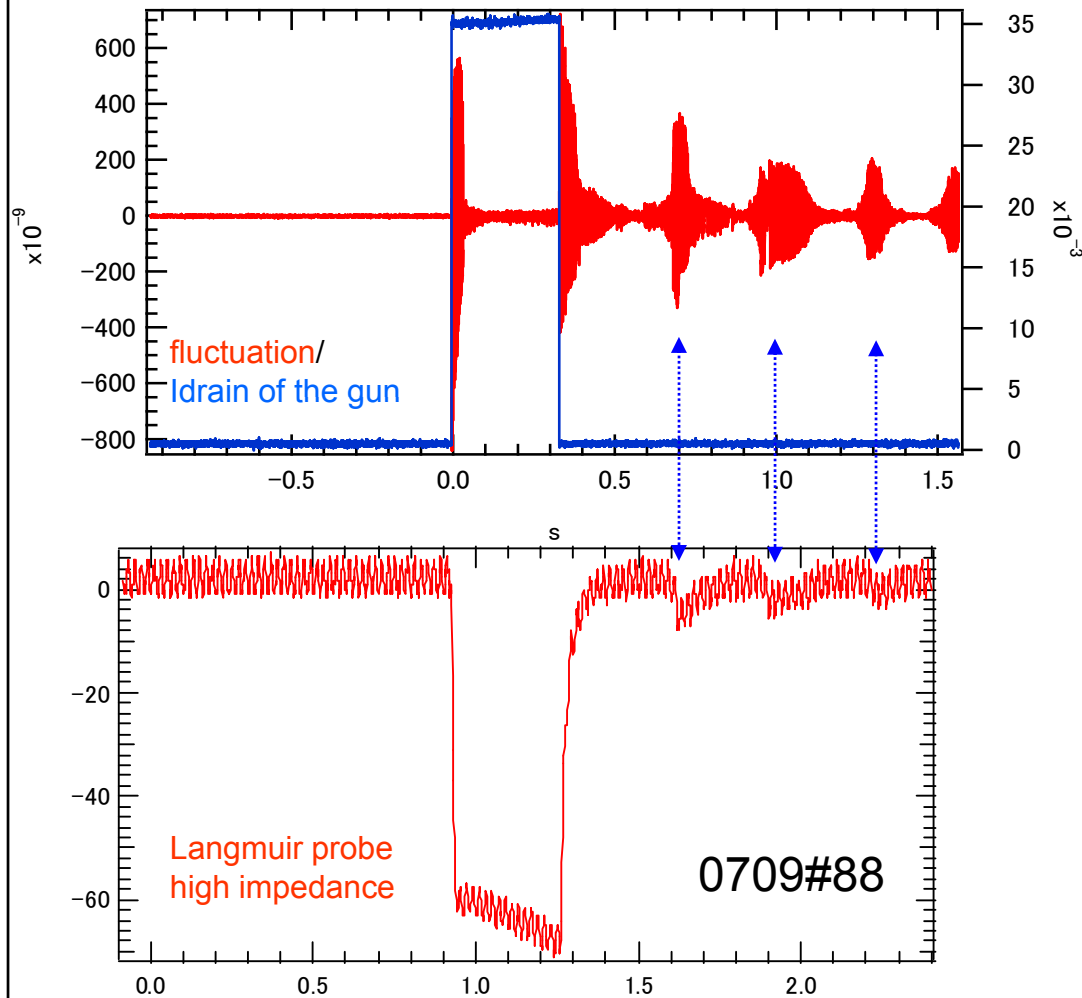


Space Potential profiles at $z=0$ cm with and without coil levitation.

- Space potential at $r < r_{gun}$ (in the stronger field region) is lower than V_{acc} , indicating inward transport and energization of electrons.
- Realized when third invariant (or canonical angular momentum) is not conserved by fluctuation, while conserving the first and second invariants.
- Flow ($E \times B$ drift in toroidal direction) has strong shear, especially when the coil is supported and the plasma has turbulence-like fluctuations.

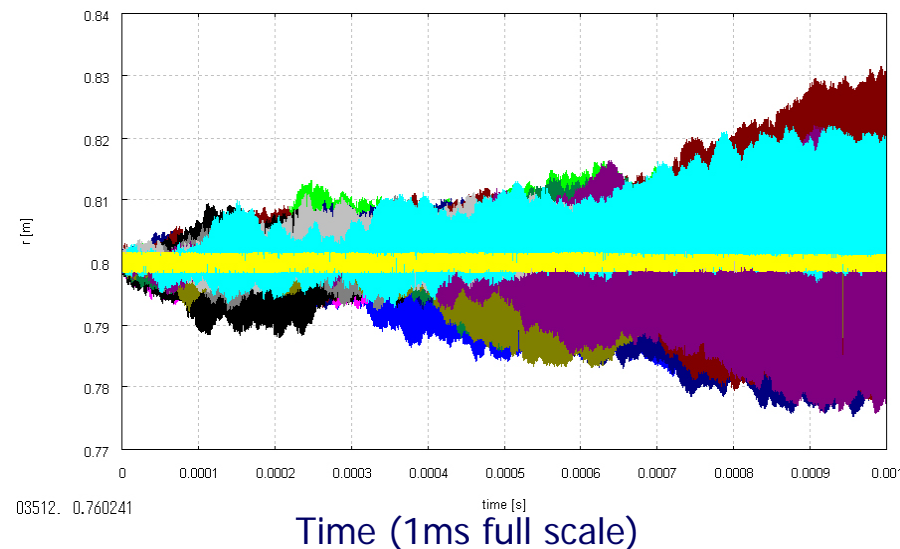
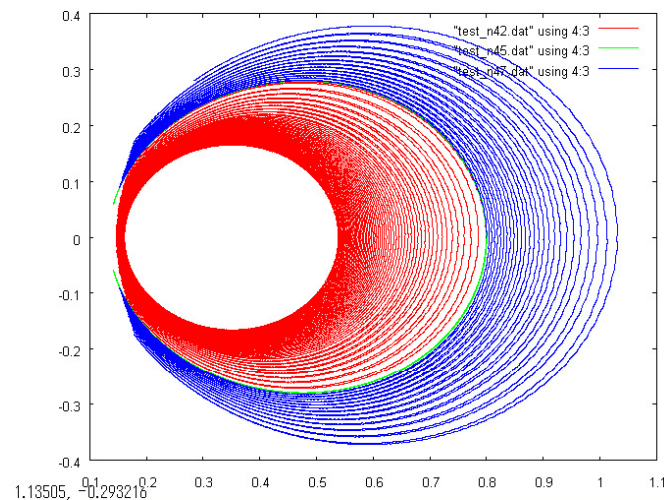
Onset of instability and radial transport

18/20



(a) Cathode voltage and fluctuation.
(b) Langmuir probe measurement.

- Radial transport and onset of instability is simultaneously observed.
- Langmuir probe was used as particle flux probe located at $r=85\text{cm}$.
- Electrons were injected from gun located at $r=80\text{cm}$.



Resonance particle orbits including azimuthal electric field of 10^4V/m
(Electron orbit for 0.01ms)

Radial transport of electrons due to random electric field.

- Toroidal symmetry was broken by adding azimuthal electric field E_θ .
- Canonical angular momentum of particle not conserved, electrons can be transported radially, violating the 3rd adiabatic invariant.
- The observed inward transport and energization of electrons can be explained by the conservations of 1st and 2nd invariants.

- Coil levitation, compensation of geomagnetic error fields, continuous discharge cleaning, resulted improved confinement in RT-1.
Ne $8 \times 10^{17} \text{m}^{-3}$ local $\beta > 40\%$ ($\sim 3.5 \text{mWb}$) $\tau_e \sim 100 \text{ms}$.
- Plasma pressure is mainly due to hot electrons. Diamag and soft x-ray measurements show $1 \sim 10 \text{keV}$ $1 - 10 \times 10^{16} \text{m}^{-3}$.
- Longtime trap of toroidal non-neutral (pure electron) plasma is realized.
Ne $1 - 10 \times 10^{11} \text{m}^{-3}$ $\tau > 300 \text{s}$ coherent and stable oscillation.
- Fluctuation-induced **inward particle diffusion** was confirmed using NNP.
 - Confinement region gradually shift to stronger field region.
 - Space potential exceed initial injection energy in strong field region.
 - Radial diffusion and onset of instability simultaneously observed.
 - Charged particles are transported inward and stably confined.
- Future tasks
 - Ion heating and formation of flowing high- β plasma.
(preliminary experiment is started)
 - Measurement of internal structure of plasma and β limitation.